Journal of Non-Newtonian Fluid Mechanics, 43 (1992) 61–82
Elsevier Science Publishers B.V., Amsterdam

Viscoelastic flow simulation using cubic stress finite elements

Rekha R. Rao [1] and Bruce A. Finlayson

Department of Chemical Engineering, BF-10, University of Washington, Seattle, WA 98195 (USA)

(Received September 5, 1991; in revised form November 15, 1991)

Abstract

The 4 : 1 axisymmetric contraction problems for Maxwell and Oldroyd-B fluids are solved using cubic finite-element interpolation for the stress field. Comparisons are made of results obtained using the explicitly elliptic momentum equation (EEME) and the inconsistent Petrov–Galerkin streamline upwinding method (SU) on unstructured triangular meshes and on structured quadrilateral meshes. Most solutions are confirmed by calculation on finer meshes, and the critical Deborah number may increase (for triangular meshes) or decrease slightly (for quadrilateral meshes) as the element size decreases.

Keywords: contraction (4 : 1); finite elements; Maxwell fluid; Oldroyd-B fluid; viscoelastic fluid flow

1. Introduction

The landmark work by Marchal and Crochet [1] introduced a novel numerical method that allowed them to obtain convergent, well-behaved solutions at a much higher Deborah number than had been reached previously. They utilized a non-consistent streamline upwinding term (SU),

Correspondence to: B.A. Finlayson, Department of Chemical Engineering, BF-10, University of Washington, Seattle, WA98195, U.S.A.

[1] Present address: Sandia National Laboratories, Division 6416, Albuquerque, NM 87185-5800, U.S.A.

0377-0257/92/$05.00 © 1992 – Elsevier Science Publishers B.V. All rights reserved

which used a Petrov–Galerkin type weight function only on the advective term in the constitutive equation (a Galerkin weighting is used for the rest of the terms), along with a four-by-four submesh for the stress field. The non-consistent weighting adds diffusion to the constitutive equation that will possibly make the equation easier to integrate near singularities in the stress field. The stress submesh gives a higher-order interpolation for the stress field, enabling it to resolve sharp gradients better. Using this method Marchal and Crochet [1] were able to solve the axisymmetric 4:1 contraction problem for essentially unlimited Deborah numbers for an Oldroyd-B fluid. They report solutions for Deborah numbers as high as 64 without a change in the sign of the Jacobian occurring in the Newton–Raphson method. The Finger strain tensor [2] remained positive definite everywhere in the fluid for Deborah numbers below 7.68. Theoretically, this tensor should be positive definite everywhere at every Deborah number when the Reynolds number is zero. For the Maxwell fluid, which is a subclass of Oldroyd-B fluids that contains no solvent, Marchal and Crochet could not achieve a convergent solution beyond a Deborah number of 7.68. However, their results were still impressive since most other reported methods have difficulty solving this problem for Deborah numbers greater than 2.

The theoretical justification for the four-by-four sub-mesh is provided by Fortin and Fortin [3], Fortin and Pierre [4], and Le Tallec [5]. Fortin and Pierre indicate that a 2×2 or 3×3 sub-mesh does not lead to a stable scheme, whereas a 4×4 sub-mesh does. They also indicate that a cubic stress space should lead to a stable scheme. Tallec describes two finite-ele-

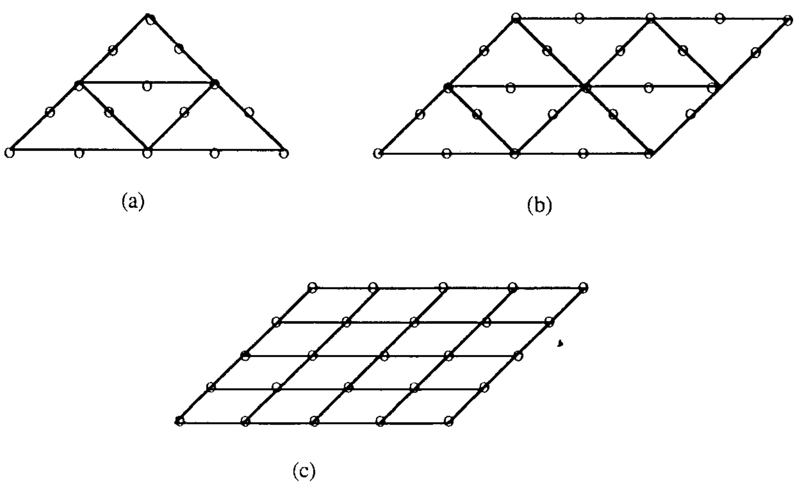

Fig. 1 Triangular mesh. (a) Subdivision into four triangles; (b) combination to form quadrilateral; (c) sub-mesh of Marchal and Crochet [1].

ment spaces that are applicable to this problem. In one finite-element space a triangular element is subdivided into four triangles in which the stress field is constant. In the other, a triangular element is subdivided into four triangles in which the stress field is biquadratic (see Fig. 1(a)). When two of the larger triangles are combined they form the mesh shown in Fig. 1(b); if the nodal points are connected in an alternate manner, they are equivalent to the four-by-four sub-mesh used by Marchal and Crochet, albeit with a different trial function for stress (see Fig. 1(c)). Marchal and Crochet [1] used a bilinear stress field on each of the sub-elements. This method treats head-on the problem of approximation of the stress field, which is governed by hyperbolic equations when the velocity is known.

Another approach to the viscoelastic flow problem is provided by King et al. [6] who employ the explicitly elliptic momentum equation (EEME). In this formulation, the stress equations and momentum equations are combined to form a revised momentum equation that retains the elliptic nature of the problem even as the Deborah number increases; they apply it to a Maxwell model.

Rao and Finlayson [7] applied the EEME to the axisymmetric 4:1 contraction problem and found that the use of EEME resulted in better solutions than could be obtained by solving the Cauchy momentum equation when quadratic polynomials are used to approximate the stress fields on each element. They also employed an adaptive mesh technique to refine the mesh in regions where the residual was high, thus employing small elements only in regions where they are needed. It had been hoped that the combination of EEME with adaptive mesh refinement would provide a method which was convergent at any Deborah number, but that proved not to be the case. The highest Deborah number for which solutions could be obtained was 3.84.

In view of the calculations reported by Marchal and Crochet [1] and the theoretical results of Fortin and Fortin [3], the study of EEME was expanded by using higher-order polynomials. In addition, the inconsistent streamline upwinding (SU) was incorporated. Finally a p-enrichment scheme was considered viable; in this method the adaption is used to select the *order* of the stress interpolation rather than the *size* of the elements. However, when the excellent results shown below became available, the plans to add the p-enrichment scheme were abandoned.

In this study, the explicitly elliptic momentum equation and the inconsistent streamline upwinding Petrov–Galerkin method are used in conjuction with finite-element spaces that are biquadratic velocity, bilinear pressure, and bicubic stress field on quadrilaterals or the equivalent spaces on triangles. We treat only the 4:1 axisymmetric contraction problem, and consider the two simplest types of fluids: a Maxwell fluid and an Oldroyd-B fluid. It is known that these two fluids are the hardest to solve since they do not undergo shear thinning. Other constitutive equations that contain shear thinning tend to reduce the stresses near the boundaries, as compared with Oldroyd-B fluids, and make the problem easier to solve.

2. Equations

The traditional equations used to model the steady, Stokes-regime flow of a viscoelastic fluid are the Cauchy momentum equation and the continuity equation

$$\nabla \cdot \boldsymbol{u} = 0, \tag{1}$$

$$\nabla p + \nabla \cdot \boldsymbol{\tau} - St \nabla^2 \boldsymbol{u} = 0, \tag{2}$$

along with a constitutive equation used to describe the viscoelastic nature of the fluid. St, the stress number, is defined as the ratio of the solvent viscosity to the polymer viscosity. It is zero for a Maxwell fluid that would be a pure polymer, and is usually taken as $St = 0.11$ for an Oldroyd-B fluid, which would be a mixture of polymer and solvent. The Maxwell model is not only the simplest available differential model, but also the model which has the lowest critical Deborah number. The Oldroyd-B model tends to have a higher critical Deborah number [8]. The solvent stress is represented in the momentum equation while the polymer stress is defined by the constitutive equation:

$$\boldsymbol{\tau} + We(\boldsymbol{u} \cdot \nabla \boldsymbol{\tau} - \nabla \boldsymbol{u}^{\mathrm{T}} \cdot \boldsymbol{\tau} - \boldsymbol{\tau} \cdot \nabla \boldsymbol{u}) = -(\nabla \boldsymbol{u} + \nabla \boldsymbol{u}^{\mathrm{T}}). \tag{3}$$

where $\boldsymbol{u}$ is the velocity, $\boldsymbol{\tau}$ is the stress, p is the pressure, and We, the Weissenberg number, is a measure of the elasticity of the fluid,

$$We = \frac{\lambda \langle u \rangle}{R}. \tag{4}$$

$\langle u \rangle$ is the average velocity of the fluid upstream, R is the downstream radius, and λ is the time constant of the polymer. The Weissenberg number differs from the Deborah number only in its non-dimensionalization:

$$De = We \dot{\gamma}_{\mathrm{w}}, \tag{5}$$

where $\dot{\gamma}_{\mathrm{w}}$ is the dimensionless downstream shear rate.

We also use a modified momentum equation designed to maintain its elliptic character, namely the explicitly elliptic momentum equation (EEME) which is formed by taking the divergence of the constitutive equation [3] and substituting in the divergence of stress from the momentum equation. After rearrangement this yields [6]:

$$\nabla \cdot (\boldsymbol{\chi} \cdot \nabla \boldsymbol{u}) + \nabla \boldsymbol{u} \cdot (\nabla \cdot \boldsymbol{\chi}) = \nabla q \tag{6}$$

where

$$q = p + We\boldsymbol{u} \cdot \nabla p, \quad \boldsymbol{\chi} = \boldsymbol{\delta} - We\boldsymbol{\tau}. \tag{7}$$

q is modified pressure and $\boldsymbol{\chi}$ is the Finger strain tensor.

3. Finite element method

Discretization with the finite-element method begins by subdividing the domain in smaller triangular or quadrilateral elements. On each element, the solution is approximated by a trial function formed by multiplying a low-order polynomial shape function with the unknown variables on the nodes of the element. The velocity is interpolated with quadratic trial functions,

$$u = \sum_{j=1}^{n} u_j N_j(r, z), \quad \text{velocity in } z\text{-direction}, \tag{8}$$

$$v = \sum_{j=1}^{n} v_j N_j(r, z) \quad \text{velocity in } r\text{-direction}. \tag{9}$$

The pressure is interpolated with a linear trial function,

$$p = \sum_{i=1}^{m} p_i N_i'(r, z) \tag{10}$$

and the stresses are represented by a cubic trial function:

$$\tau_q = \sum_{k=1}^{p} \tau_{qk} N_k''(r, z). \tag{11}$$

The subscript q denotes the zz, zr, rr components of the stress tensor or its trace. The formulae for the linear, quadratic, and cubic Lagrangian shape functions can all be found in Zienkiewicz [9].

The trial functions are next substituted into the equations of interest to form the residual equations. The residual equations are multiplied by a weight function and integrated over the region of the problem; the resulting non-linear algebraic equations are solved with the Newton–Raphson method.

Two different types of weight functions are utilized for this work. The most common weight functions used are of the Galerkin type, where the shape functions themselves are used to weight the residual equations. Thus, the continuity equation is weighted with the linear shape function, the momentum equation is weighted with the quadratic shape function, and the stress equation is weighted with the cubic shape function.

The other weight function used is for a non-consistent streamline upwinding, with only minor changes to the traditional Galerkin weighting. In this case, a Petrov–Galerkin weighting is used only on the advective term of the stress equation, $\boldsymbol{u} \cdot \nabla \boldsymbol{\tau}$, with a Galerkin weighting on all other terms. The general form of the SU weight function is

$$W_j(r, z) = N_j''(r, z) + C_e \frac{u \dfrac{\partial N_j}{\partial z} + v \dfrac{\partial N_j}{\partial r}}{u^2 + v^2}$$
$$= N_j''(r, z) + WPG_j(r, z), \quad (12)$$

where W_j is the Petrov–Galerkin weighting, N_j'' is the cubic shape function, and C_e is an element constant defined below. We abbreviate the upwind part of the Petrov–Galerkin weighting by WPG_j. As the velocity approaches zero, the weighting function WPG_j approaches a function of position which is independent of velocity, at least when using eqn. (13) or (14) below. Since the velocity was never zero, no special precautions were taken when dividing by the magnitude of velocity.

Marchal and Crochet [1] define C_e as

$$C_e = \frac{\left[(v_\xi h_\xi)^2 + (v_\eta h_\eta)^2\right]^{1/2}}{2}, \quad (13)$$

where u_ξ is the velocity at the centroid in the direction ξ, v_η is the velocity at the centroid in the direction η, h_ξ is the size of the element measured from the center of the element in the ξ direction, and h_η is the size in the η direction. Note that in the original paper presenting streamline upwinding by Brookes and Hughes [10], they say that the value of the coefficient is not as important as the structure of the SU function.

Here a modified version of C_e is used because of the unstructured nature of our triangular meshes. It is not obvious for a triangle where the natural η and ξ directions are, because triangles have three natural coordinates, so instead we use the norm of the centroid velocity multiplied by the approximate element size. Crochet's formulation is denoted SU. This second version is called SU1, where the modified coefficient is defined as

$$C_e' = \frac{(u_0^2 + v_0^2)^{1/2}(h_\xi^2 + h_\eta^2)^{1/2}}{2}, \quad (14)$$

where u_0 is the velocity at the centroid in the x-direction and v_0 is the velocity at the centroid in the y-direction. The third choice of C_e yields SU2, which uses only the approximate element size as the coefficient without any centroid velocities.

$$C_e'' = \frac{(h_\xi^2 + h_\eta^2)^{1/2}}{2}. \quad (15)$$

The choice of this formulation proved to be serendipitous: when we were testing the Newton–Raphson computer codes, we set the centroid velocity term to unity and got surprisingly good results.

The application of the streamline upwind weighting to eqn. (3) gives

$$\left\{\boldsymbol{\tau}^{\mathrm{h}} + We\left(\boldsymbol{u}^{\mathrm{h}} \cdot \boldsymbol{\nabla}\boldsymbol{\tau}^{\mathrm{h}} - \boldsymbol{\nabla}\boldsymbol{u}^{\mathrm{hT}} \cdot \boldsymbol{\tau}^{\mathrm{h}} - \boldsymbol{\tau}^{\mathrm{h}} \cdot \boldsymbol{\nabla}\boldsymbol{u}^{\mathrm{h}}\right) + \left(\boldsymbol{\nabla}\boldsymbol{u}^{\mathrm{h}} + \boldsymbol{\nabla}\boldsymbol{u}^{\mathrm{hT}}\right);\ N_j''\right\}$$
$$+ \left\{We\boldsymbol{u}^{\mathrm{h}} \cdot \boldsymbol{\nabla}\boldsymbol{\tau}^{\mathrm{h}};\ WPG_j\right\} = 0. \tag{16}$$

By working backwards from eqn. (16), we find the actual differential equation we are solving with a Galerkin method:

$$\boldsymbol{\tau} + We\left(\boldsymbol{u} \cdot \boldsymbol{\nabla}\boldsymbol{\tau} - \boldsymbol{\nabla}\boldsymbol{u}^{\mathrm{T}} \cdot \boldsymbol{\tau} - \boldsymbol{\tau} \cdot \boldsymbol{\nabla}\boldsymbol{u}\right) = -\left(\boldsymbol{\nabla}\boldsymbol{u} + \boldsymbol{\nabla}\boldsymbol{u}^{\mathrm{T}}\right) + \boldsymbol{\nabla} \cdot (\boldsymbol{\beta} \cdot \boldsymbol{\nabla}\boldsymbol{\tau}),$$
$$\boldsymbol{\beta} = WeC_{\mathrm{e}} \frac{\boldsymbol{u}\boldsymbol{u}}{(\boldsymbol{u} \cdot \boldsymbol{u})}. \tag{17}$$

We can see that this modified stress equation is the standard Maxwell model (3) with the addition of a diffusion term, $\boldsymbol{\nabla} \cdot (\boldsymbol{\beta}\boldsymbol{\nabla}\boldsymbol{\tau})$.

While Marchal and Crochet [1] used this added term as a numerical artifact arising from the streamline upwinding method, El-Kareh and Leal [11] noted that exactly such a diffusion term has been left out of the derivation of most constitutive equations derived from kinetic theory. By including such a term in a FENE dumbbell model, they were able to prove the existence of solutions to their constitutive equation at all values of the Deborah number. Thus the addition of a non-consistent streamline upwind term is not just an arbitrary numerical technique, but many actually have some physical significance.

High-order Gaussian integration must be used to calculate the integrals caused by discretization with the finite-element method for the cubic interpolants so that integration error does not pollute the solution. Very accurate quadrature is necessary because of the high-order (perhaps rational) polynomial order of the Petrov–Galerkin weighting function. (This is one area where the use of lower-order polynomials on a sub-mesh is advantageous.) A variety of quadrature methods were tested from 7th-order to 15th-order. Solutions shown here used 7th-order quadrature on triangles [12,13] and 9th-order Gaussian quadrature on quadrilaterals [14].

The set of differential equations is converted to a set of algebraic equations by use of the finite-element method. This set of non-linear equations is solved using the Newton–Raphson method. In the case of SU1 it was found best to use a successive substitution method for the weighting function itself. The weighting function depends on the solution, and it was evaluated with SU1 by using the solution at the previous iteration rather than by expanding the weighting function in a Newton–Raphson method.

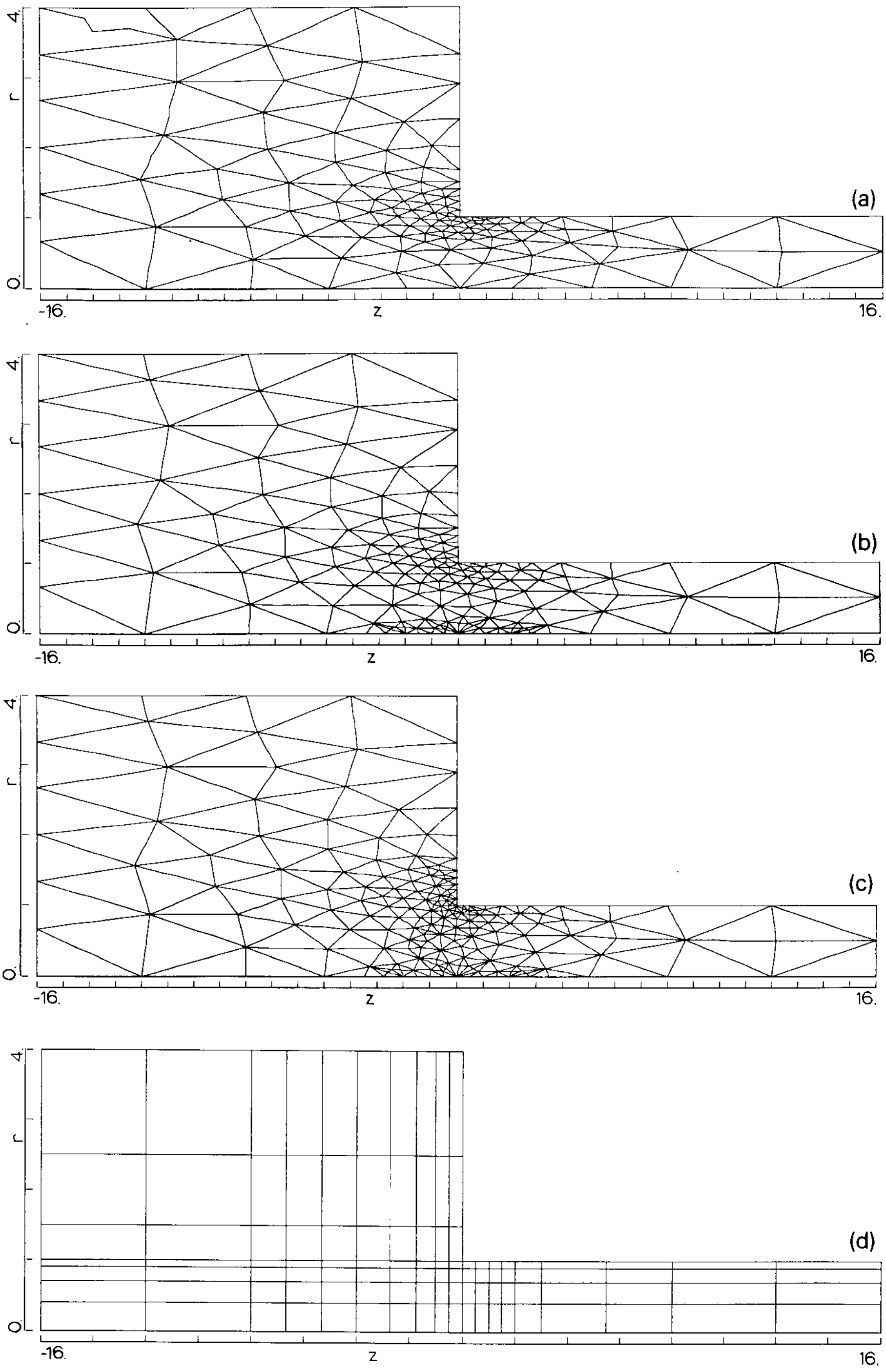

Fig. 2. Meshes. (a) Initial mesh; (b) centerline-refined mesh; (c) centerline-and-singularity-refined mesh; (d) quadrilateral mesh; (e) refined quadrilateral mesh; (f) long quadrilateral mesh; (g) long, refined quadrilateral mesh.

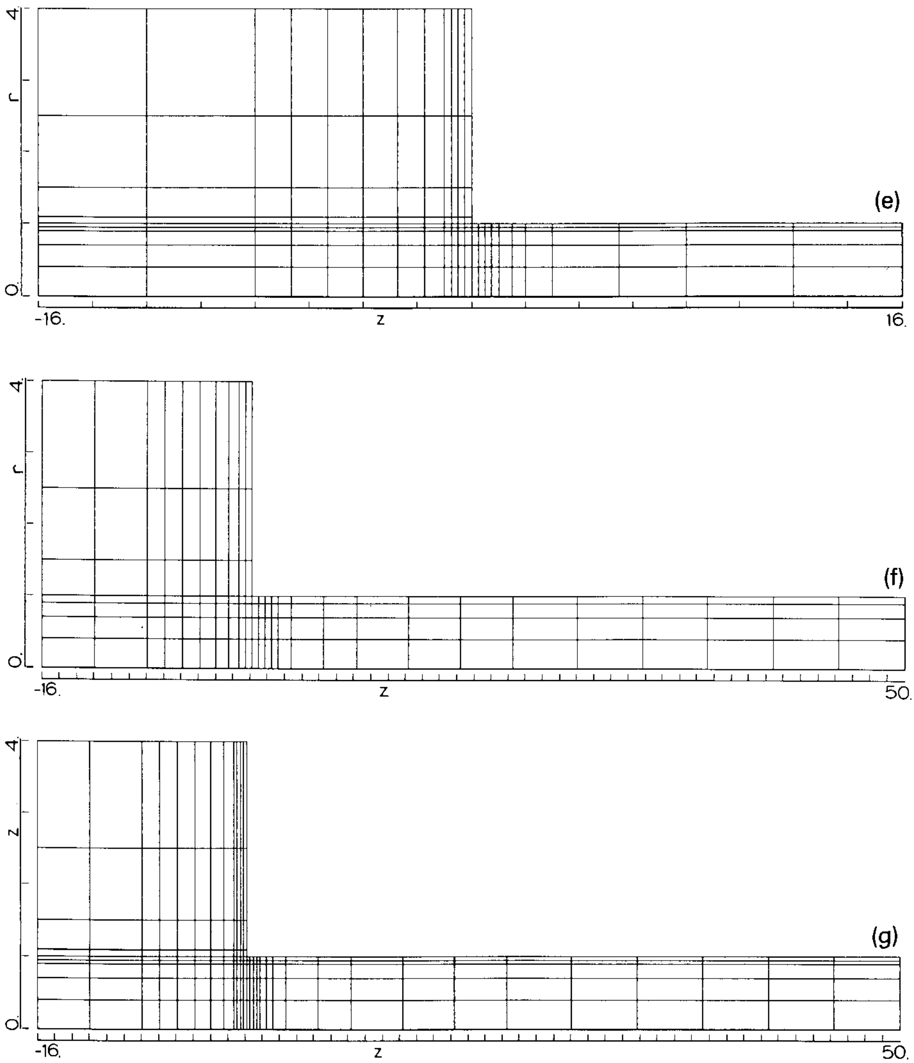

Fig. 2 (continued).

We used a full Newton–Raphson method on all terms with SU2, as did Marchal and Crochet [1].

Obviously there are several choices to be made: to use EEME or not, to use streamline upwinding or not, and if it is used which formulation of SU to use, and on which mesh to perform the calculations. While all combinations have not been explored, more complete results than presented here are available in Rao's thesis [15]. The results presented here are ones that give good quality solutions that have been confirmed on finer meshes. We can say at the outset that the Galerkin method with cubic stress fields, without EEME or SU, did not work well at all; the solutions were actually worse than those obtained with quadratic stress fields. Thus no solutions are presented here for the Galerkin method in its unadulterated version.

When using triangular finite elements, results are shown on three meshes (Figs. 2(a)–2(c)). The first mesh was obtained with an interactive mesh generation program, the second was derived by refining the initial mesh around the centerline. The third mesh was obtained from the second mesh by adaptively refining the Newtonian solution. This tends to add elements near the corner where there is a singularity (see Rao and Finlayson [16] for details of the mesh refinement scheme).

The coarse quadrilateral mesh is shown in Fig. 2(d) and is the same one used by Josse [17]. The element at the corner has a size of length 0.1 in the radial direction and 0.5 in the axial direction. This mesh was refined by making smaller elements near the singularity, obtaining the mesh shown in Fig. 2(e). This mesh has lengths of 0.05 and 0.25 in the radial and axial directions, respectively. At high Deborah numbers, a longer distance downstream from the contraction is required for the fluid to rearrange into a fully developed profile. The longer meshes are shown in Fig. 2(f) and 2(g).

4. Numerical results

4.1 Maxwell fluid

Results are first described for a Maxwell fluid. Since there is no shear thinning for this model, it applies to real fluids only at very low shear rates; it is a hypothetical model at high shear rates. However, the methods which are successful for a Maxwell fluid can be applied to other fluids. Unfortunately, it is also the most difficult fluid to simulate at high shear rates.

The effect of the choice of equations can be demonstrated by listing the critical Deborah number. The problem was always solved for a Newtonian fluid, and then the Deborah number was increased in steps. Usually first-order continuation was used, but sometimes zeroth-order continuation proved more successful. In zeroth-order continuation the initial guess is the solution for a slightly smaller Deborah number. In order to do a first-order continuation, we solve for the solution and its derivative with respect to Deborah number. Then the initial guess is the solution for a slightly smaller Deborah number plus the derivative times the change in Deborah number. The step-size was varied in an attempt to achieve solutions at as high a Deborah number as possible. Thus the critical Deborah number is subject to some uncertainty, since it may depend on the past history of the iterative solution. The critical Deborah numbers on the initial mesh are listed in

TABLE 1

Critical Dcborah numbers on the initial mesh

Weight function	Equation	Critical *De*	DOF [a]	Mcsh
Galerkin	CME	1.92	5300	2a
Galerkin	EEME	2.56	5300	2a
SU1	CME	3.20	5300	2a
SU1	EEME	5.76/5.76/7.04	5300/6555/8071	2a/2b/2c
SU2	CME	19.2/17.9	5219/7886	2d/2e

[a] Degrces of freedom.

Table 1. The Galerkin solutions have the lowest critical Deborah number; when the EEME is used the critical Deborah number increases. It also increases if SU1 is used, and takes the highest value if both SU1 and EEME are used.

The critical Deborah number is also compared when SU1 and EEME are used together for different meshes. The critical Deborah numbers are 5.76, 5.76, and 7.04 on meshes 2a/2b/2c. Thus the critical Deborah number increases with mesh refinement for the unstructured meshes. This is a necessary test which any successful method must pass. The solutions are compared for a Deborah number of 5.76 in Figs. 3 and 4. Figures 3(a)–3(c) show the contours of the *zz*-stress on the three meshes. All the solutions are acceptable, but the solution without extraneous wiggles in the contours is the one on the finest mesh. The *zz*-stress along the plane of the contraction ($r = 1$) is shown in Figs. 4(a)–4(c). All three solutions capture the essential features, but again the results are best for the finest mesh. Thus the results converge with mesh refinement with SU1/EEME at a Deborah number of 5.76.

Turning next to results obtained on the quadrilateral mesh, we found that SU2 worked best with a full Newton–Raphson iteration. Results are shown only for the Cauchy momentum equation (the EEME option was not tried). On mesh 2d the critical Deborah number was 19.2, whereas on mesh 2e it was 17.92. In this case, the critical Deborah number did not increase with mesh refinement, but the numbers are close. Solutions at a Deborah number of 16.64 are shown in Figs. 5(a)–5(d). The solutions are very similar upon mesh refinement. This Deborah number is considerably larger than any reported in the literature for a Maxwell fluid.

The results for the Maxwell fluid indicate that the method is confirmed on finer meshes, but it still has an upper limit in Deborah number. However, the Deborah number is considerably larger than reported previously. The SU1/EEME on triangles and SU2/CME on quadrilaterals give

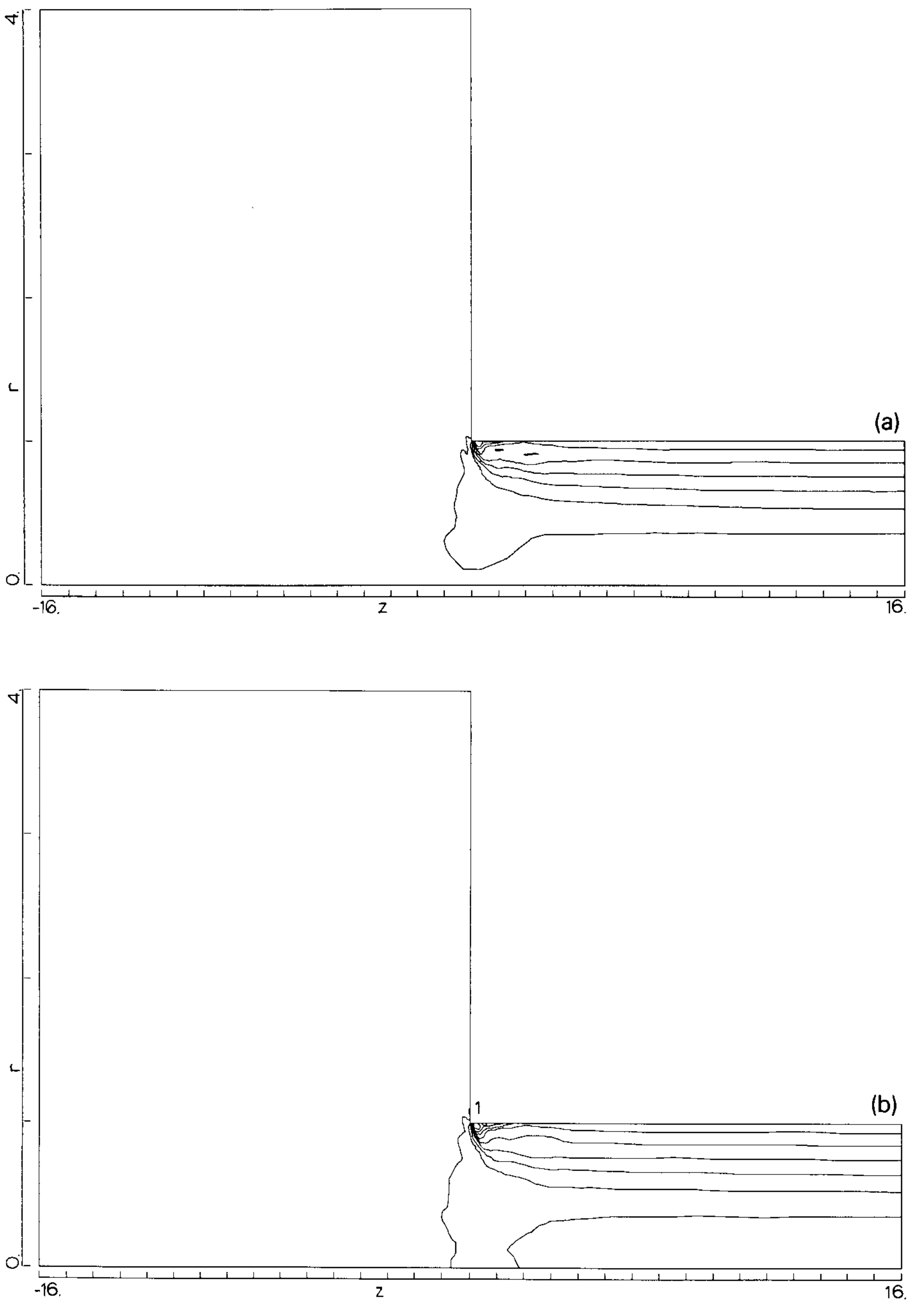

Fig. 3. *zz*-Stress contours for SU1/SS weight function and EEME for $De = 5.76$ and a Maxwell fluid; (a) mesh 2a; (b) mesh 2b; (c) mesh 2c.

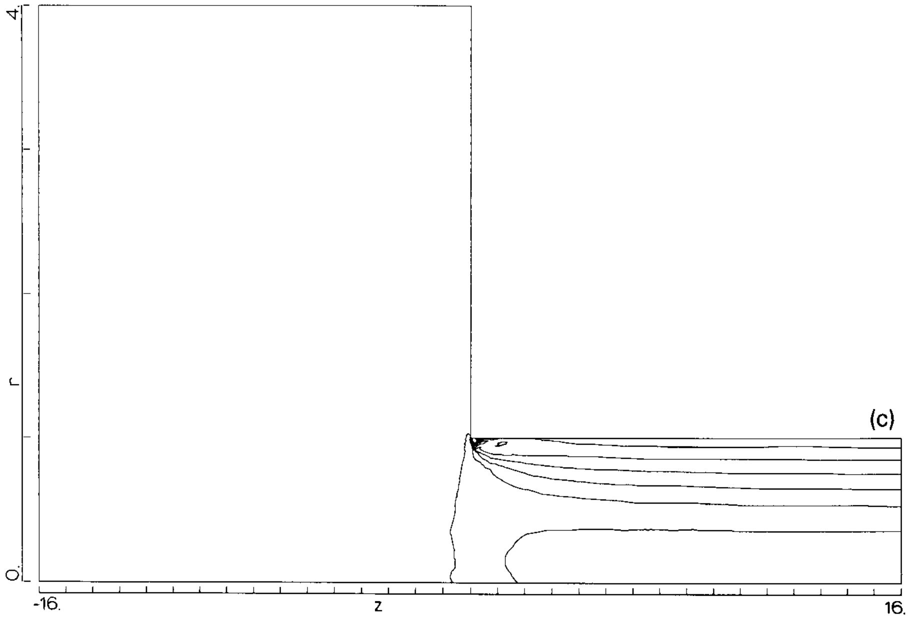

Fig. 3 (continued).

excellent results. The highest Deborah numbers were achieved on structured meshes.

4.2 Oldroyd-B fluid

The SU1/CME option was employed for an Oldroyd-B fluid, too. The EEME formulation is more difficult to implement for an Oldroyd-B fluid, because of the appearance of third derivatives of velocity; thus we do not employ this option here.

The critical Deborah number increased from 5.76 to 7.68 when going from mesh 2a to mesh 2c. The solutions were also good at the critical Deborah number (see Figs. 6(a)–6(b)). Better results were obtained for quadrilateral meshes. On mesh 2d the critical Deborah number was 41.3, whereas it was only 29.4 for the mesh 2e. For Deborah numbers this large, a longer mesh was needed. On mesh 2f the critical Deborah number was 42.2 but the solutions quality was excellent.

Results for a Deborah number of 42.2 were generated using SU2/CME on mesh 2f. The streamlines are shown in Fig. 7, while the plots of zz-stress field on the plane of the contraction ($r = 1$), and the zz-stress and axial velocity on the centerline are shown in Figs. 8(a)–8(c). These solutions are excellent and demonstrate the ability of the finite-element method using streamline upwinding (SU2) and cubic stress interpolation to solve this problem on regular, structured meshes.

5. Discussion

Marchal and Crochet [1] used a method with non-consistent streamline upwinding and a four-by-four sub-mesh approximation of the stress. In

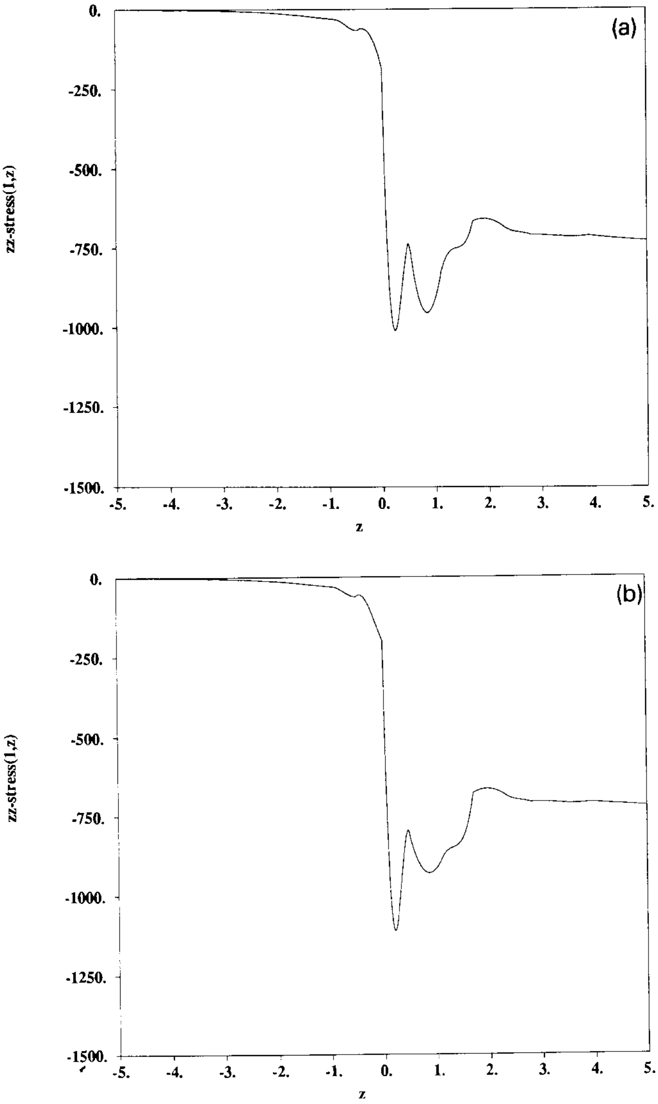

Fig. 4. zz-Stress in the plane of the contraction ($r=1$, $-5 \leq z \leq 5$) for SU1/SS weight function and EEME for $De=5.76$ and a Maxwell fluid; (a) mesh 2a; (b) mesh 2b; (c) mesh 2c.

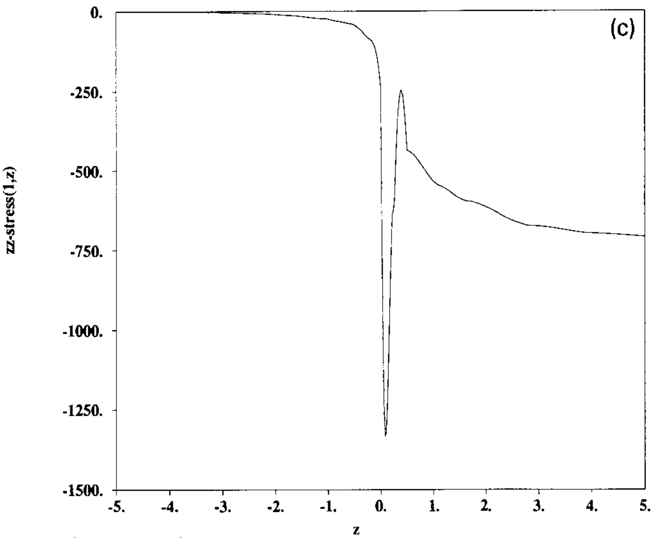

Fig. 4 (continued).

contrast, we use cubic polynomials for stress (which is similar to a three-by-three sub-mesh) and a slightly different weighting function in the streamline upwinding. The work of Fortin and Pierre [4] indicates that both methods should lead to convergent results.

5.1 Maxwell fluid

Marchal and Crochet could not achieve a convergent solution beyond a Deborah number of 7.68, and do not report calculations on different meshes. On unstructured meshes we, too, were limited to a Deborah number of 7.04, although this was achieved on the finest mesh (2c). On structured meshes, though, we were able to reach a Deborah number of 18 or 19, even when the mesh was refined. The three differences between our work and that of Marchal and Crochet are: using SU2 instead of SU (eqn. (15) instead of eqn. (13)), using a slightly different mesh, and using cubic polynomials for stress interpolation instead of a 4×4 bilinear sub-mesh. Only the last item is significantly different.

5.2 Oldroyd-B

Marchal and Crochet [1] concentrated on calculations for an Oldroyd-B fluid. When their corner element was 0.092 by 0.092 they did calculations up to a Deborah number of 64 without observing a change of sign in the Jacobian. Results up to 7.68 resulted in a positive definite stress tensor.

They refined their mesh, giving a corner element of size 0.05 by 0.05 and did calculations up to a Deborah number of 20, with no reported reason to stop other than disinterest. On this mesh the stress tensor, ***TA***, was positive definite everywhere when the Deborah number was less than or equal to

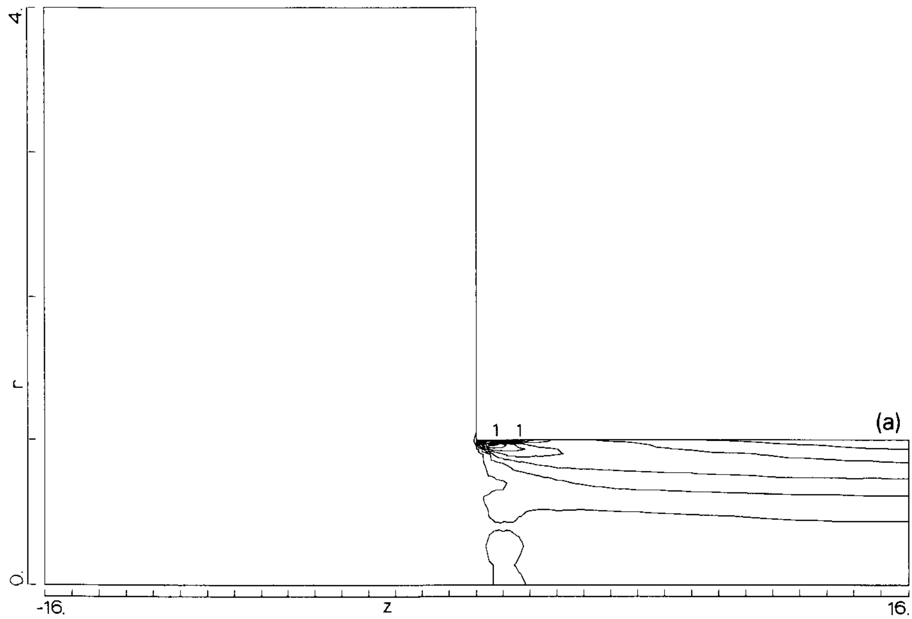

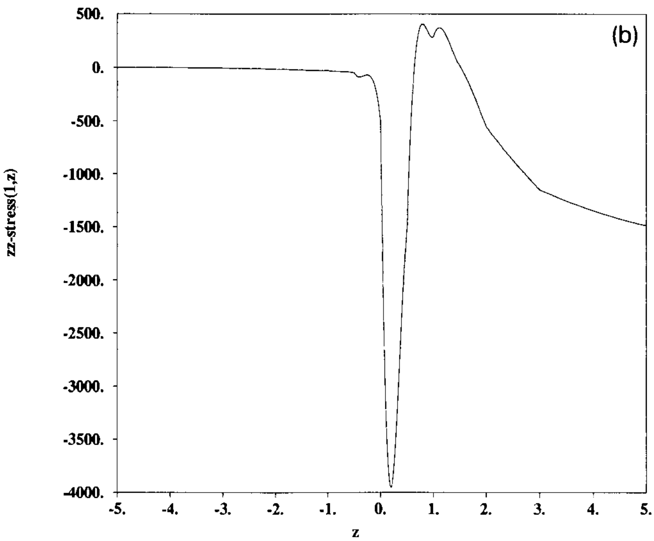

Fig. 5. *zz*-Stress for SU2/NR weight functions and CME and a Maxwell fluid, $De = 16.64$; (a, b) mesh 2d; (c, d) mesh 2c; (b and c along $r = 1$).

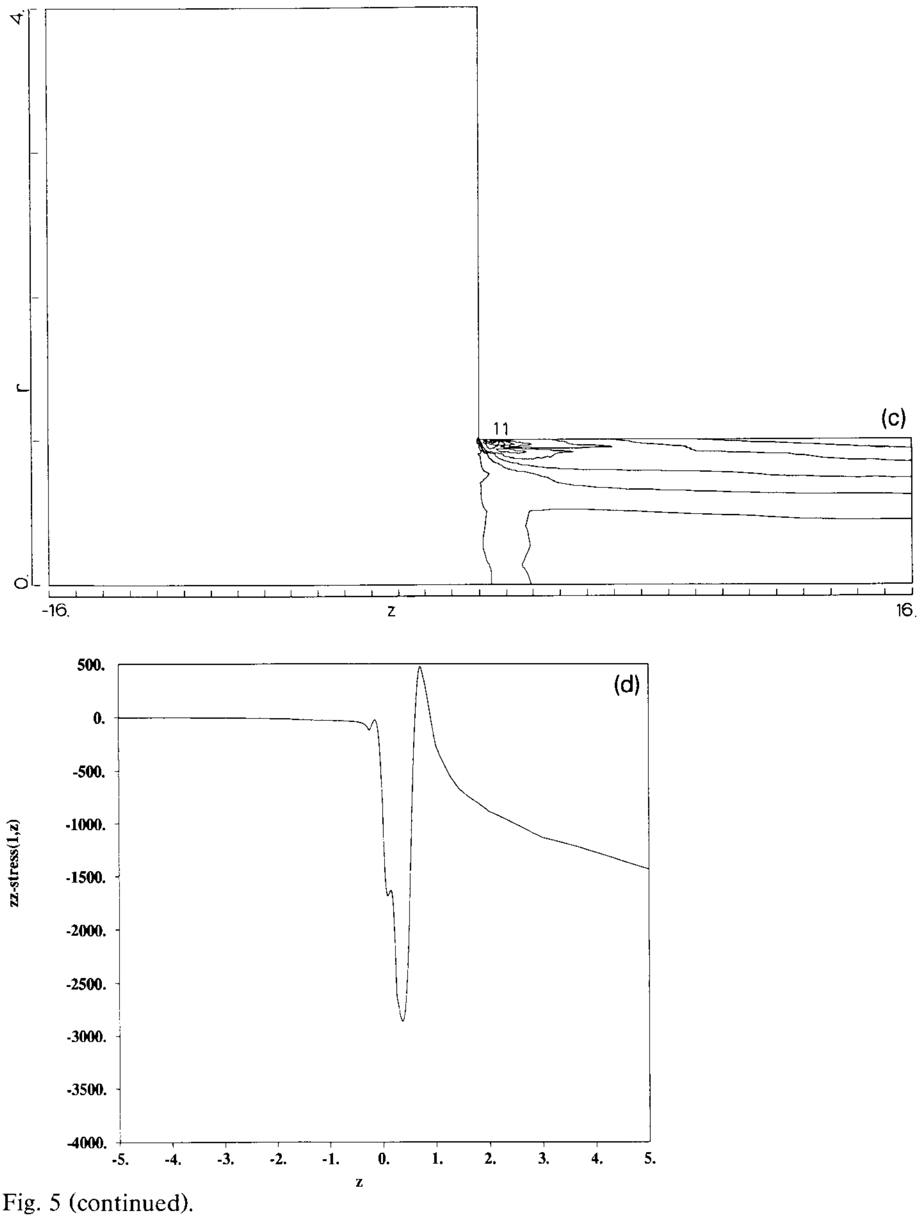

Fig. 5 (continued).

7.2. Thus, they confirmed solutions with mesh refinement for a Deborah number of 20 and calculated (on one mesh) up to a Deborah number of 64. We confirmed solutions with mesh refinement for a Deborah number of 26 and calculated (on one mesh) up to a Deborah number of 41. We did reach un upper limit, however, while Marchal and Crochet did not. Our solutions

(Figs. 7, 8(a)–8(c)) are virtually identical to those of Marchal and Crochet (their Figs. 25 and 26, respectively).

We also found the choice of streamline upwinding weighting function important, in that all options did not work for triangular meshes. However,

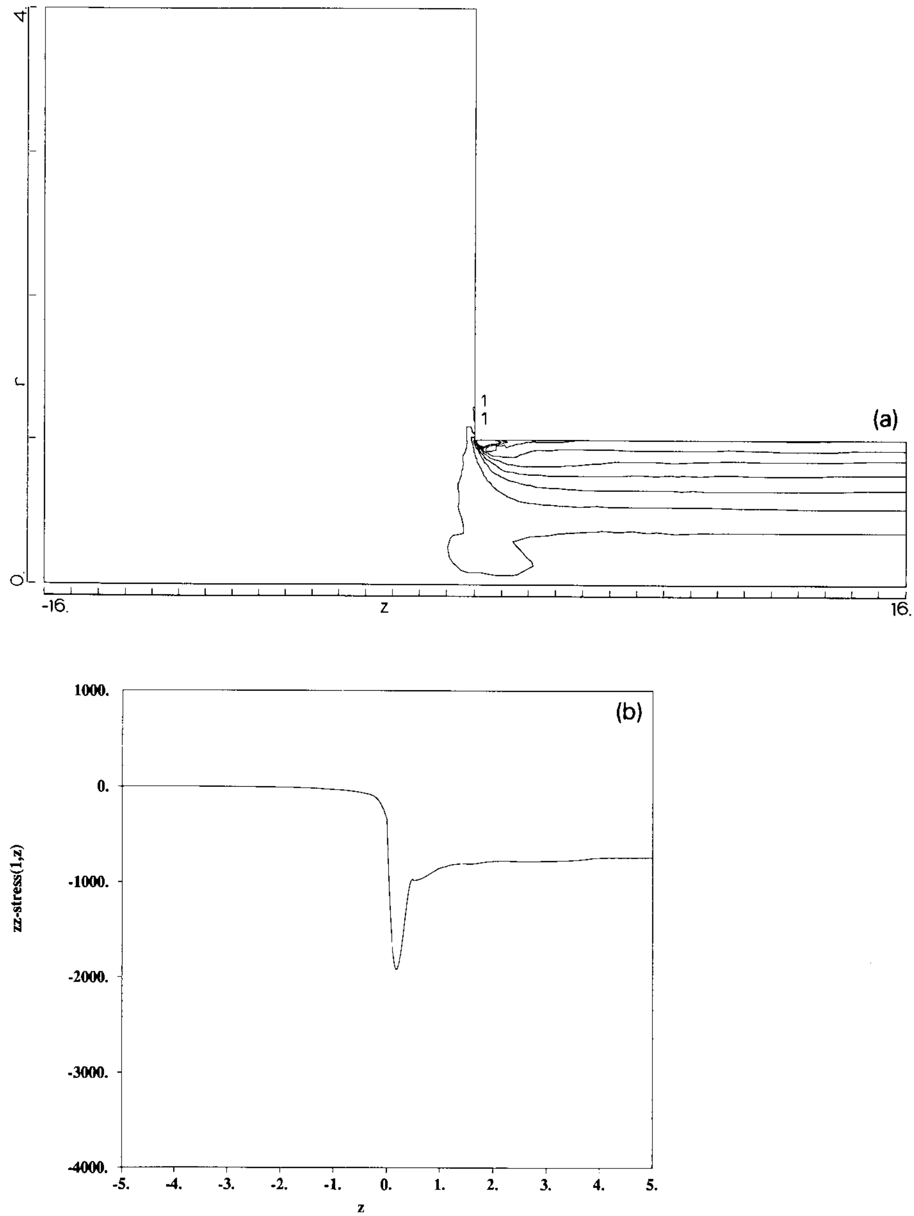

Fig. 6. *zz*-Stress for SU1/SS weight function and CME on mesh 2c for Oldroyd-B fluid; (a, b) $De = 7.04$; (c) $De = 7.68$; (b and c along $r = 1$).

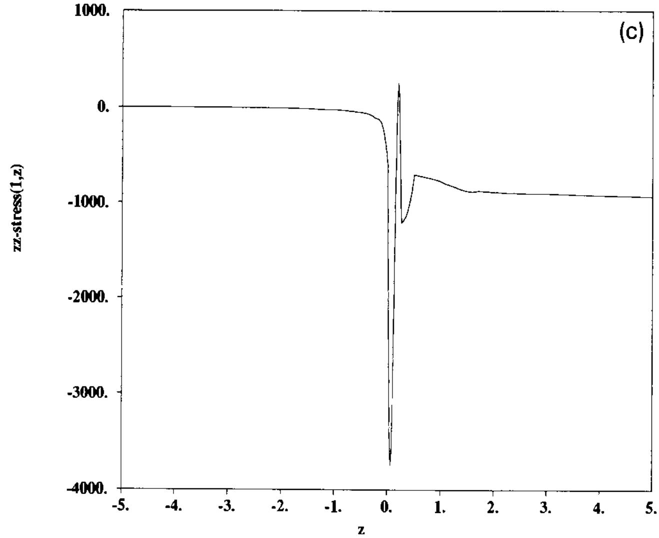

Fig. 6 (continued).

one method worked best on triangles and another method worked best on quadrilaterals, and the solutions were not significantly different. We hypothesize that the weighting function that works is closely tied to the upstream nature of the calculation, and that the use of cubic trial functions is probably not the best choice. Marchal and Crochet specifically chose a four-by-four sub-mesh since the Petrov–Galerkin method had been developed for low-order trial functions. The results presented here show that many of the same results can be achieved using cubic trial functions. It would be interesting to repeat the study using quartic polynomials, since they are most closely related to the four-by-four sub-mesh used by Marchal

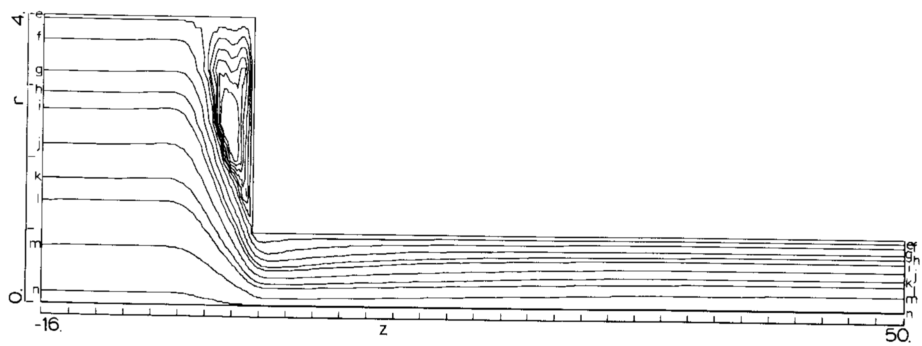

Fig. 7. Streamlines, $De = 42$, SU2/NR weight function and CME on mesh 2f for Oldroyd-B fluid; contours at: $n = -0.032$, $m = -0.63$, $l = -1.9$, $k = -2.7$, $j = -4.1$, $i = -5.5$, $h = -6.2$, $g = -7.0$, $f = -7.6$, $e = -7.9$.

and Crochet, but the work was ended before the p-enrichment scheme was implemented.

6. Conclusions

The use of cubic polynomials to represent the stress components in this finite-element simulation is definitely preferred over the use of quadratic

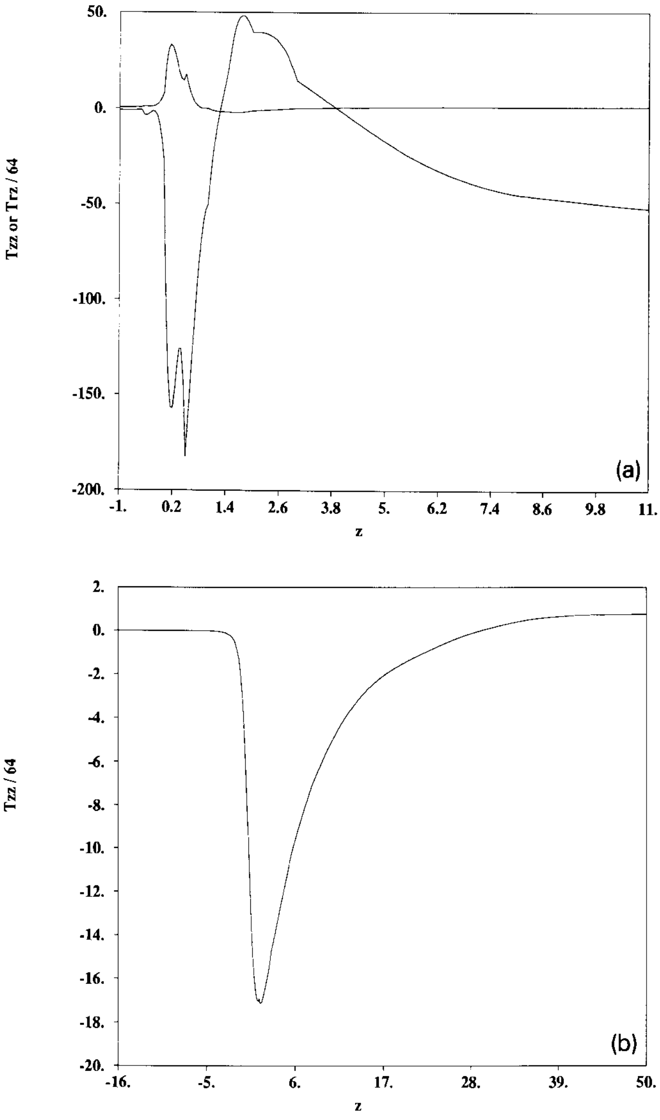

Fig. 8. Stress and velocity, $De = 42$, SU2/NR weight function and CME on mesh 2f for Oldroyd-B fluid; (a) zz-stress and rz-stress along line $r = 1$; (b) zz-stress along line $r = 0$; (c) axial velocity along line $r = 0$.

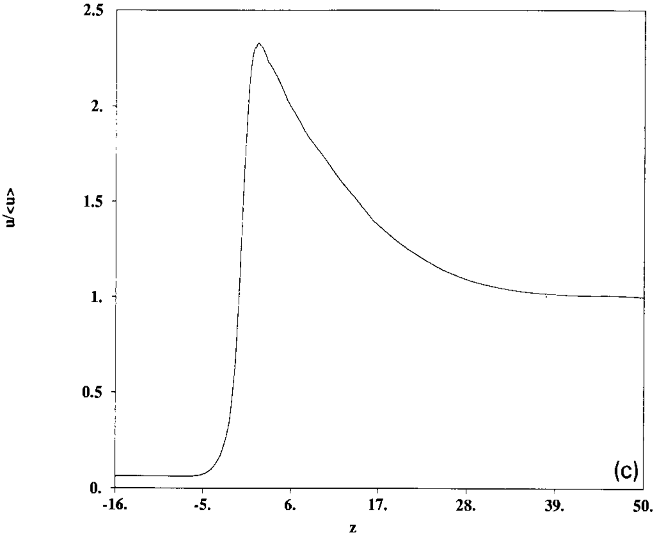

Fig. 8 (continued).

or linear polynomials. For the axisymmetric 4:1 contraction problem, with either Maxwell fluids or Oldroyd-B fluids, good solutions could be obtained with cubic polynomials and either streamline upwinding or the explicitly elliptic momentum equation, or both. These solutions were confirmed on finer meshes. A critical Deborah number was found, and this number increased upon mesh refinement when triangles were used but not when quadrilaterals were used. (We note that Marchal and Crochet [1] also did not confirm their calculations for their highest Deborah number on a finer mesh.) The highest Deborah number for which calculations were successful was 19.2 for a Maxwell fluid and 42 for an Oldroyd-B fluid; these were achieved on structured meshes. The use of streamline upwinding is best for structured meshes, and apparently is best for low-order bilinear sub-meshes, which leads to no apparent critical Deborah number [1]. The problem can be solved using unstructured triangular meshes with the cubic approximation for stress components and either streamline upwinding or the explicitly elliptic momentum equation, or both. While results on unstructured meshes are of good quality, a lower critical Deborah number was achieved compared with results for structured meshes.

References

1 J.M. Marchal and M.J. Crochet, A new mixed finite element for calculating viscoelastic flow, J. Non-Newtonian Fluid Mech., 26 (1987) 77–114.
2 R.B. Bird, R.C. Armstrong and O. Hassager, Dynamics of Polymeric Liquids, Vol. 1, Fluid Mechanics, Wiley-Interscience, New York, 1987, p. 427.

3 M. Fortin and A. Fortin, A new approach for the FEM simulation of viscoelastic flows, J. Non-Newtonian Fluid Mech., 32 (1989) 295–310.
4 M. Fortin and R. Pierre, On the convergence of the mixed method of Crochet and Marchal for viscoelastic flows, Comput. Methods Appl. Mech. Eng., 73 (1989) 341–350.
5 P. Le Tallec, Numerical Analysis of Viscoelastic Problems, Masson, Springer-Verlag, Berlin, 1990.
6 R.C. King, M.R. Apelian, R.C. Armstrong and R.A. Brown, Numerically stable finite element techniques for viscoelastic calculations in smooth and singular geometries, J. Non-Newtonian Fluid Mech., 29 (1988) 147–216.
7 R.R. Rao and B.A. Finlayson, Adaptive refinement of a viscoelastic flow problem with the explicitly elliptic momentum equation, J. Non-Newtonian Fluid Mech., 38 (1991) 223–246.
8 M.J. Crochet, Numerical simulation of viscoelastic flow: a review, Rubber Chem. Technol., 62 (1989) 426–455.
9 O.C. Zienkiewicz, The Finite Element Method, 3rd edn., McGraw-Hill, London, 1977.
10 A.N. Brooks and T.J.R. Hughes, Streamline upwind/Petrov–Galerkin formulations for convection-dominated flows with particular emphasis on the incompressible Navier–Stokes equations, Comput. Methods Appl. Mech. Eng., 32 (1982) 199–259.
11 A.W. El-Kareh and L.G. Leal, Existence of solutions for all Deborah numbers for a non-Newtonian model modified to include diffusion, J. Non-Newtonian Fluid Mech., 33 (1989) 257–287.
12 G. Lague and R. Baldur, Extended numerical integration method for triangular surfaces, Int. J. Num. Methods Eng., 11 (1977) 388–392.
13 J.N. Lyness and D. Jespersen, Moderate degree symmetric quadrature rules for the triangle, J. Inst. Maths. Applics., 15 (1975) 19–32.
14 A.H. Stroud and D. Secrest, Gaussian Quadrature Formulas, Prentice Hall, Englewood Cliffs, NJ, 1966.
15 R.R. Rao, Adaptive finite-element analysis of non-Newtonian flow, Ph. D. Thesis, University of Washington, 1990.
16 R.R. Rao and B.A. Finlayson, On the quality of viscoelastic flow solutions: an adaptive refinement study of a Newtonian and a Maxwell fluid, Int. J. Num. Methods Fluids, 11 (1990) 571–585.
17 S. Josse, Contraction flow of viscoelastic fluids, Ph. D. Thesis, University of Washington, 1986.